Evidence That Eosin-5-maleimide Binds Close to the Anion Transport Site of Human Erythrocyte Band 3: A Fluorescence Quenching Study†

Rui-jun Pan and Richard J. Cherry*

Department of Chemistry and Biological Chemistry, University of Essex, Wivenhoe Park, Colchester CO4 3SQ, U.K.

Received August 9, 1994; Revised Manuscript Received January 26, 1995®

ABSTRACT: The interaction between eosin-5-maleimide (EMA), an inhibitor of the anion transport protein, band 3, and I^-, a transportable substrate, was investigated by fluorescence quenching. The Stern−Volmer plot for the quenching reaction between EMA-labeled band 3 and I^- exhibits downward curvature both in human erythrocyte ghosts and in purified band 3. The quenching reaction is insensitive to the viscosity of the bulk phase. The shape of the Stern−Volmer plot becomes more linear with increasing temperature. Following the approach of Blatt *et al.* [(1986) *Biophys. J. 50,* 349−356], we have developed a binding-diffusion model which is in good agreement with the quenching data. The model supposes that EMA is located in a compartment or "pocket" in band 3 which is separate from the bulk phase and contains a binding site or sites for the quencher. Quenching of band 3-bound EMA fluorescence by I^- is inhibited by DIDS and by the transportable anions Cl^-, HCO_3^-, and Br^-. Analysis of these experiments yields dissociation constants for the anions which are in reasonable agreement with those determined from transport kinetics and by NMR. We thus deduce that the quencher binding site is the anion binding/transport site on band 3. We propose that EMA is located in the wall of the anion access channel such that it does not inhibit anion binding. The methods described in this report should facilitate detailed studies of anion binding to the transport site on band 3 under a variety of experimental conditions.

Band 3 (M_r = 95 000−101 000) is the most abundant protein of the human red cell membrane. It comprises ~25% (by weight) of the total membrane protein and is present at ~10^6 copies per cell [for reviews, see Reithmeier (1993) and Salhany (1990)]. Band 3 is an anion transporter which can be structurally and functionally divided into two distinct domains. The 42 kDa hydrophilic cytoplasmic domain of band 3 provides binding sites for the membrane cytoskeletal proteins, hemoglobin, and some glycolytic enzymes (Low, 1986). The membrane-spanning domain of band 3 contains the anion transport function and is believed to span the bilayer up to 14 times in the form of α-helices (Jennings, 1985; Kopito & Lodish, 1985; Tanner *et al.*, 1988; Wood, 1992). The membrane-spanning domain can be further digested by chymotrypsin into two fragments, a 17 kDa N-terminal fragment and a 35 kDa C-terminal fragment (Salhany, 1990). There are several pieces of evidence favoring that both 17 kDa and 35 kDa fragments are directly and/or allosterically involved in the one-to-one anion exchange across the membrane (Salhany *et al.*, 1987; Jennings *et al.*, 1984; Bar-Noy & Cabantchik, 1990).

Much information concerning band 3 structure and function has been derived from chemical modification studies, particularly of the binding site for the stilbenedisulfonate class of anion transport inhibitors. The site can be reached by stilbenedisulfonates only from the extracellular solution (Kaplan *et al.*, 1976) and is located in a cleft that extends some distance from the outer surface of the membrane, as indicated by fluorescence resonance energy transfer estimates of the distance between the stilbenedisulfonate site and the cytoplasmic domain (Rao *et al.*, 1979). This notion was also supported by a more recent report that inhibitors conjugated to macromolecules are denied access to the transport site of band 3 from either membrane surface unless they are spaced out by narrow aliphatic chains (Eidelman *et al.*, 1991). The reversible stilbenedisulfonates are competitive inhibitors of anion exchange (Shami *et al.*, 1978; Fröhlich, 1982). Thus, it is generally believed that the exofacial anion transport site is contained in the stilbenedisulfonate site (Passow, 1986; Fröhlich & Gunn, 1978; Wojciki & Beth, 1993), although some results suggest that the mechanism of chloride and reversible stilbenedisulfonate binding to band 3 involves separate but interacting sites (Dix *et al.*, 1986; Salhaney *et al.*, 1994). Two lysine residues have been identified at the stilbenedisulfonate site. Lys-A is Lys-539 (Bartel *et al.*, 1989a,b) on the 17 kDa fragment, and the other lysine residue, Lys-B, is Lys-851 on the 35 kDa fragment (of the human protein sequence) (Kopito & Lodish, 1985; Wood *et al.*, 1992; Okubo *et al.*, 1994). At higher pH, DIDS[1] can covalently react with both lysine residues to form an intramolecular cross-link (Jennings & Passow, 1979; Salhany, 1990). However, neither Lys-A nor Lys-B is absolutely necessary for anion transport (Passow, 1986; Passow *et al.*, 1992; Jennings *et al.*, 1985).

Among other probes such as pyridoxal 5′-phosphate (PLP), NAP-taurine, and arginine-, histidine-, and glutamate-specific

† R.P. was supported by the British Council.

* To whom correspondence should be addressed.

® Abstract published in *Advance ACS Abstracts,* March 15, 1995.

[1] Abbreviations: DIDS, 4,4′-diisothiocyanatostilbene-2,2′-disulfonic acid disodium salt; EMA, eosin-5-maleimide; NAP-taurine, *N*-(4-azido-2-nitrophenyl)-2-aminoethanesulfonate; NH_3-TEMPO, 4-amino-2,2,6,6-tetramethylpiperidine-1-oxyl; PLP, pyridoxal 5′-phosphate; PMSF, phenylmethanesulfonyl fluoride; S-V plot, Stern−Volmer plot; BSA, bovine serum albumin; SDS, sodium dodecyl sulfate; 5PB, 5 mM sodium phosphate, pH 7.8; PBS, 5 mM sodium phosphate, 150 mM NaCl, 1 mM EDTA, pH 7.8; 310 buffer, 90 mM disodium hydrogen phosphate, 20 mM sodium dihydrogen phosphate, pH 7.5.

0006-2960/95/0434-4880$09.00/0

reagents (Julien & Zaki, 1988; Hamasaki *et al.*, 1989; Jennings & Anderson, 1987) which have been used to identify the transport site, eosin derivatives have attracted much attention for two reasons. One is that, because of its long triplet-state lifetime (~2 ms), eosin-5-maleimide (EMA) has been extensively used to study the rotational dynamics of band 3 by laser-induced transient dichroism (Cherry, 1979, 1992) and by phosphorescence anisotropy measurements (Austin *et al.*, 1979; Tilley & Sawyer, 1992) and also to monitor band 3 conformational changes (Wyatt & Cherry, 1992). The other reason is that EMA is a specific inhibitor of band 3 anion transport. Almost complete inhibition occurs at a molar ratio of 1:1 (EMA:band 3 monomer), and the labeling is prevented by previous incubation of intact erythrocytes with DIDS (Nigg *et al.*, 1979; Nigg & Cherry, 1979). Thus studies to characterize the binding site of EMA on band 3 as well as inhibition kinetics are of considerable interest in relation to band 3 structure and function.

Both protein chemistry and site-directed mutagenesis studies of band 3 have identified Lys-430 (human sequence) as the amino acid residue with which EMA covalently reacts (Cobb & Beth, 1990; Passow *et al.*, 1992). It is reported that Lys-430 is conserved in all members of the anion-exchange family so far studied but is not essential for anion exchange (Passow *et al.*, 1992). From hydropathy plots, it is predicted that Lys-430 is located on the extrafacial loop connecting the first and second transmembrane segments (Reithmeier, 1993).

Although the EMA covalent binding site on the primary structure of band 3 is known, the topological location of the eosin moiety in band 3 and the role of the EMA binding site in the anion transport function remain to be elucidated. Macara *et al.* (1983) observed that EMA bound covalently to band 3 at the extracellular side is only accessible to the fluorescence quencher, Cs^+, from the intracellular side. They proposed that covalent labeling by EMA induces a conformational change of band 3 with the eosin moiety lying deep in the transport pocket close to the intracellular surface of the membrane. Wyatt and Cherry (1992), however, found that I^- can only quench the triplet state of EMA bound to band 3 from the extracellular side. The mutual exclusion of DIDS and EMA labeling suggests that EMA when bound to band 3 lies in the transport pocket (Nigg *et al.*, 1979; Nigg & Cherry, 1979; Macara & Cantley, 1981), but Knauf and co-workers observed that EMA inhibits Cl^- exchange in a noncompetitive fashion and hence proposed that the EMA binding site is not at the band 3 transport site (Knauf *et al.*, 1993; Liu & Knauf, 1993).

In the present study, fluorescence quenching of EMA by I^- is used to further investigate the location of EMA on band 3. As well as acting as a quencher, I^- is a high-affinity transported substrate anion, although with a relatively low transport rate [for review, see Knauf (1979)]. Since the fluorophore EMA is not only a photochemical probe but also a specific inhibitor of anion transport, it is possible to probe the transport domain of band 3 by measuring fluorescence quenching of band 3-bound EMA by I^-. The experimental results presented in this paper are shown to be consistent with a binding-diffusion model of I^- fluorescence quenching. Moreover, competition studies with other transported anions enable dissociation constants for these anions to be determined.

MATERIALS AND METHODS

Materials. Eosin-5-maleimide was obtained from Molecular Plobes, Inc., DIDS was from Pierce Chemical Co., and NH_3-TEMPO and BSA were from Sigma. Triton X-100 was from Boehringer-Mannheim, Brij 58 from Aldrich, and DEAE-cellulose from Whatman. All other reagents used were of the highest grade available.

Labeling of Band 3 with EMA and Preparation of Ghosts. Band 3 was selectively labeled with EMA as described by Nigg and Cherry (1979). Briefly, erythrocytes were washed 3 times in 5 mM sodium phosphate, 150 mM NaCl, and 1 mM EDTA, pH 7.8 (PBS). Cells were washed once in 310 mosM phosphate buffer, pH 7.5 (310 buffer) and then incubated with EMA (1 mg of EMA in 2 mL of 310 buffer for every 5 mL of packed cells) in the dark at room temperature for 45 min. After being washed in PBS three more times, the labeled cells were lysed in 30 volumes of 5 mM sodium phosphate, pH 7.8 (5PB) containing 20 μg/mL PMSF and 1 mM EDTA. Ghosts were then prepared by centrifuging the lysed cells at 40000*g* for 15 min at 4 °C until the supernatant was clear.

Protein was determined by the Lowry method (Lowry *et al.*, 1951) after the ghosts were solubilized in 1% SDS, and the EMA concentration was determined by measuring absorbance at 531 nm. The stoichiometry of labeling was calculated assuming band 3 accounts for 25% of the total membrane protein and taking the extinction coefficient for band 3-bound EMA to be 83 000 M^{-1} cm^{-1} (Cherry, 1978). A typical molar ratio of EMA:band 3 was 1:1. Ten percent SDS−polyacrylamide gel electrophoresis was used routinely to check the specificity of labeling.

Isolation of Band 3. Purification of band 3 was performed as described by van Veen and Cherry (1992). The EMA-labeled ghosts were preextracted in 1% Brij 58 and then solubilized with 5 volumes of 50 mM NaCl/10 mM Tris-HCl, pH 8.0, containing 0.5% (w/w) Triton X-100 for 30 min. The residual membrane and the cytoskeleton were pelleted by centrifugation at 40000*g* for 30 min, and subsequently solubilized band 3 protein was applied to a DE52 cellulose column preequilibrated with 50 mM NaCl/10 mM Tris-HCl, pH 8.0. The elution buffer contained 250 mM NaCl, 10 mM Tris-HCl, and 0.5% Triton X-100 (pH 8.0). Eluted EMA-labeled band 3 fractions were identified by the pink color of EMA, and the isolated protein was dialyzed against 5 mM sodium phosphate and 0.5% Triton X-100, pH 7.8. All procedures were carried out at 4 °C in the dark.

EMA Labeling of Other Proteins. BSA was labeled with EMA by incubation with the probe at 1 mg of EMA/40 mg of BSA in PBS at room temperature for 45 min. To remove free EMA, the labeling solution was passed through a filtration membrane (Amicon PM10), and then the concentrated BSA solution was dialyzed against 5PB. Eosin-labeled spectrin was kindly provided by I. E. G. Morrison.

Fluorescence Quenching Titration. Fluorescence intensities were determined on a Baird Nova spectrofluorometer. Eosin was excited at 505 nm, and the emission was recorded at 547 nm with excitation and emission slits adjusted to 2.5 nm. Eosin concentration was generally ~10^{-7} M.

Quenching titrations were performed by measuring the fluorescence of EMA−band 3 in ghosts before and after addition of KI from a freshly prepared stock solution

consisting of 4 M KI with ~2 mM $Na_2S_2O_3$ to prevent formation of I_3^- (Macara *et al.*, 1983). For each quencher concentration, the ghosts were suspended in 5PB buffer containing an amount of trisodium citrate such that after addition of different amounts of I^- the ionic strength remained constant at 250 or 350 mM depending on the highest concentration of iodide used. Fluorescence intensities were corrected for the small dilution factor (<5%) arising from the addition of the quencher stock solution.

Model Simulation and Curve Fitting. All simulation and curve fitting were performed with "Ultrafit", a nonlinear curve-fitting package written for Macintosh (from BIOSOFT, Cambridge, U.K.). The fitting algorithm employed was the Levenberg–Marquardt method. The quality of the fitting was evaluated by the goodness-of-fit index P, which is calculated from the incomplete γ function using χ^2 statistics and the number of degrees of freedom. In all curve-fitting calculations we obtained $P = 1$, which indicates an excellent fit.

THEORY

Derivation of Binding-Diffusion Quenching Model. A simple diffusional quenching reaction in solution is described by the standard Stern–Volmer equation:

$$F_0/F - 1 = K_{SV}[Q] \tag{1}$$

where F_0 and F are the fluorescence intensities in the absence and presence of quenchers, K_{SV} is the quenching constant, and [Q] is the quencher concentration in the bulk solution. In complex systems, the above equation requires modification. Blatt *et al.* (1986) have previously analyzed quenching in membranes and other compartmentalized systems on the basis of both partitioning and saturable binding of the quencher. Here we extend their approach to the case of a fluorophore which is located in a compartment separate from the bulk solution such as the active site of an enzyme or the transport channel of a membrane protein. We suppose that the compartment or "pocket" in which the fluorophore is situated also contains a binding site or sites for the quencher.

For a fluorophore located in a pocket, the quenching efficiency will depend on $[Q]_e$, the effective quencher concentration in the pocket, where

$$[Q]_e = \langle Q \rangle / V_P \tag{2}$$

and thus

$$F_0/F - 1 = K_{SV}\langle Q \rangle / V_P \tag{3}$$

where $\langle Q \rangle$ is the average number of quencher molecules per pocket and V_P is the molar volume of the pocket.

If the distribution of quencher molecules between the bulk and the pocket is mediated by an affinity binding process, then

$$\langle Q \rangle = ([Q]_t - [Q]_f)/[R] \tag{4}$$

and

$$\langle Q \rangle = n[Q]_f/(K_d + [Q]_f) \tag{5}$$

where $[Q]_f$ is the bulk concentration, [R] is the concentration of the pocket structure, n is the number of quencher binding sites per pocket, and K_d denotes the dissociation constant of the quencher molecules binding in the pocket (note that, for simplicity, identical binding sites are assumed).

Derivation of an expression for $[Q]_f$ in terms of the total quencher concentration, $[Q]_t$, from eqs 4 and 5 leads to a quadratic function. Under the condition that $[Q]_t \gg n[R]$, however, then approximately $[Q]_f = [Q]_t$ and from eqs 3 and 5 we obtain

$$F_0/F - 1 = (nK_{SV}/V_P)([Q]_t/(K_d + [Q]_t) \tag{6}$$

or

$$F_0/F - 1 = K_q[Q]_t/(K_d + [Q]_t) \tag{7}$$

where $K_q = nK_{SV}/V_P$ is the apparent diffusion quenching constant. Under saturation conditions (i.e., $[Q]_t \gg K_d$), the fluorescence of the sample will reach a constant value, F_s, given by

$$F_0/F_s - 1 = K_q \tag{8}$$

We now apply the model to I^- quenching of band 3-bound EMA and assume only one I^- binding site per pocket. If we define P_x as the fraction of binding sites occupied by I^-, then

$$P_x = [I^-]/(K_d + [I^-]) \tag{9}$$

At subsaturation concentrations, the fraction P_x of EMA–band 3 will have fluorescence F_s while the fraction $(1 - P_x)$ will not be quenched and hence have fluorescence F_0. Thus the total fluorescence of the sample will be

$$F = (1 - P_x)F_0 + P_xF_s \tag{10}$$

and from eqs 8–10 we obtain

$$F_0/F - 1 = K_q[I^-]/(K_d(1 + K_q) + [I^-]) \tag{11}$$

Inhibition of I^- Binding-Diffusion Quenching by Competing Anions. We now consider the situation where a second, nonquenching anion competes for the I^- binding site. The fraction of sites that are occupied by I^-, (P_i), is

$$P_i = [XI^-]/[X]_t \tag{12}$$

where $[XI^-]$ is the concentration of the bound I^- and $[X]_t$ is the total concentration of binding sites given by

$$[X]_t = [X] + [XA] + [XI^-] \tag{13}$$

Here [XA] is the concentration of the bound anion A which competes with I^-, and [X] is the concentration of free sites. [XA] and $[XI^-]$ can be written in terms of the dissociation constants K_d^A and K_d and the free reactant concentrations [X], [A], and $[I^-]$, respectively:

$$[XI^-] = [X][I^-]/K_d \tag{14}$$

$$[XA] = [X][A]/K_d^A \tag{15}$$

Substitution of eqs 13–15 into eq 12 gives

$$P_i = [I^-]/\{([A]/K_d + 1)K_d^A + [I^-]\} \tag{16}$$

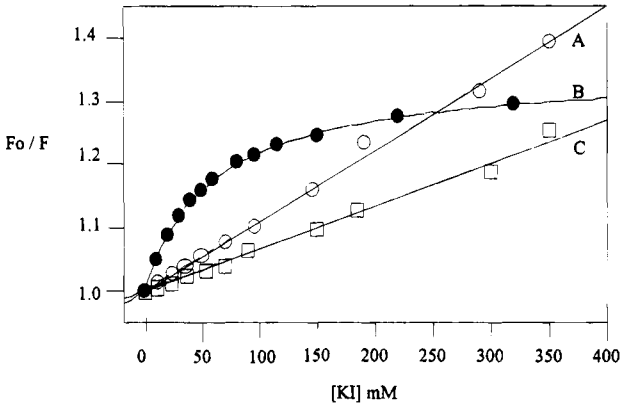

FIGURE 1: Stern–Volmer plots of I^- quenching of the fluorescence of EMA bound to different proteins: (●) EMA-labeled erythrocyte ghosts (EMA bound to band 3); (○) EMA-labeled spectrin; (□) EMA-labeled BSA. All measurements were carried out in 5PB with varying amounts of trisodium citrate to maintain the ionic strength constant at 350 mM. [EMA] was 10^{-7} M; temperature, 14 °C.

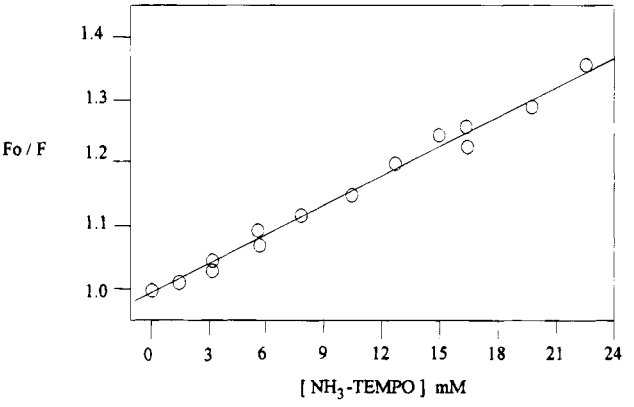

FIGURE 2: Stern–Volmer plot of NH_3-TEMPO quenching of the fluorescence of band 3-bound EMA in ghosts. The data were fitted by a linear least squares procedure to eq 1 in Theory. The best-fit parameters are K_{SV} = 53 M^{-1} (correlation coefficient = 0.985). The quenching titration was performed in 5PB containing 28.5 mM trisodium citrate, pH 7.8 at 14 °C.

By comparison with eq 9, it can be seen that, in the presence of a competing anion, the apparent dissociation constant, K_d', for I^- binding becomes

$$K_d' = ([A]/K_d^A + 1)K_d \qquad (17)$$

Thus, a plot of K_d' against [A] is linear, and K_d^A can be determined from the slope.

RESULTS AND ANALYSIS

Characteristics of Fluorescence Quenching of EMA–Band 3 by I^-. Figure 1 shows the results of I^- quenching of fluorescence of ghosts derived from EMA-labeled intact erythrocytes. It is noteworthy that the S-V plot exhibits downward curvature. Figure 1 also shows I^- quenching of EMA covalently bound to the purified erythrocyte skeletal protein, spectrin, and to BSA. For these proteins, the S-V plot is linear. In addition, when a nitroxide spin label, NH_3-TEMPO, is used to quench EMA–band 3, a linear S-V plot is also obtained (Figure 2). These results indicate that the downward curvature of the S-V plot is characteristic of the particular quenching reaction and depends on the macromolecule to which EMA conjugated.

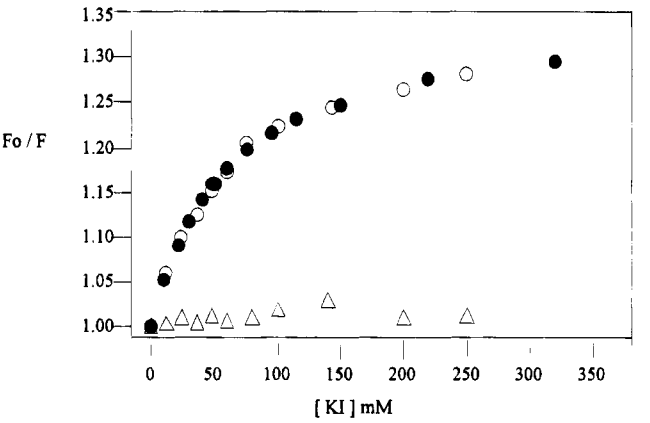

FIGURE 3: Effects of nonionic and anionic detergents on the quenching reaction between EMA-labeled band 3 and I^-: (●) EMA-labeled ghosts; (○) purified EMA-labeled band 3 in the presence of 0.5% (w/w) Triton X-100; (△) EMA-labeled ghosts solubilized in 1% (w/w) SDS. All measurements were carried out in 5PB at 14 °C. The ionic strength was maintained at 350 mM by addition of trisodium citrate.

Similar quenching experiments were also performed with ghost membranes solubilized with nonionic and anionic detergents. It was found that solubilization in 1% (w/w) SDS protected band 3-bound EMA from quenching by I^- but purification in 0.5% (w/w) Triton X-100 produced no observable change in the quenching reaction (Figure 3). The latter result agrees with previous studies indicating that band 3 retains its native conformation in nonionic detergent micelles (Jennings, 1984; Casey & Reithmeier, 1993). The protection against quenching in SDS is probably due to electrostatic repulsion of I^- by the negatively charged surface of the micelle.

There are a number of possible explanations of the downward-curving S-V plot which involve heterogeneity of either the eosin binding site or the morphology of the membrane preparation. Bar-Noy and Cabantchik (1990), for example, reported downward-cuving S-V plots for acrylamide quenching of the fluorescence of PLP, a band 3 affinity label, in both inside-out and right-side-out vesicles. They attributed this result to inhomogeneity in their vesicle preparations. The observation that the same downward-curving S-V plot is obtained with purified band 3 in Triton X-100 micelles, however, rules out any effect of membrane heterogeneity in the present case. This result also eliminates the possibility of interference by other proteins, in agreement with the fact that EMA labeling of intact cells is highly specific for band 3.

It is highly unlikely that there are multiple eosin binding sites on band 3 since it has been independently reported that eosin labels a single site, Lys-430 (Macara *et al.*, 1983; Cobb & Beth, 1990; Passow *et al.*, 1992). A further possibility is that although all EMA binds to the same residue on band 3, it can nevertheless adopt more than one conformation in its binding site. This again seems a highly unlikely explanation because if this were the case, the S-V plot would imply that a large fraction of eosin is inaccessible to I^-. Quenching by the larger NH_3-TEMPO molecule, however, shows no evidence of such a large heterogeneity and indeed yields a linear S-V plot (Figure 2). As a further check for possible heterogeneity, the fluorescence spectrum and fluorescence polarization (p) were determined for band 3-bound EMA in the absence and presence of quencher. The two spectra were

identical, and the values of $p = 0.376 \pm 0.011$ (no quencher) and $p = 0.372 \pm 0.016$ (350 mM KI) exhibited no significant difference. These results show that the curved S-V plot is not due to a second eosin binding site which is relatively inaccessible to quencher.

The present results also cannot be explained by static quenching which produces an upward-curving S-V plot. Macara *et al.* (1983) did observe saturable static quenching of band 3-bound EMA by Cs^+. Because they found that Cs^+ did not quench eosin in free solution or bound to BSA, they suggested that the inability to obtain 100% quenching is an intrinsic property of the quencher−fluorophore interaction. The results in Figure 1 show that the present results cannot be explained along these lines.

Binding-Diffusion Model for I^- Quenching of Band 3-Bound EMA. An alternative explanation of the obseved downward-curving S-V plot is that fluorescence quenching by I^- involves two distinct steps, namely, binding from the bulk solution to a site or sites on band 3 followed by diffusion to reach the fluorophore. Blatt *et al.* (1986) have previously presented an analysis of fluorescence quenching in membranes which includes a saturable binding step. We have followed their approach to develop a binding-diffusion model for I^- quenching of band 3-bound EMA (see Theory). The notion that the eosin probe is located within a pocket in band 3 is supported by the fact that band 3-bound EMA is strongly protected from triplet-state quenchers in the aqueous phase (Wyatt & Cherry, 1992) and from fluorescence resonance energy transfer experiments which show that the probe is deeply embedded in the protein (Macara *et al.*, 1983).

When the concentration of quencher in the pocket is determined by a binding step, the S-V plot exhibits downward curvature arising from saturation of the binding sites (eq 11). The derivation of eq 11 assumes that $[Q]_t \gg n[R]$; this condition is satisfied in the present study where the working concentration for band 3 was on the order of 10^{-7} M and the concentration of quencher was on the order of 10^{-1} M.

To further investigate the applicability of the binding-diffusion model, the temperature dependence of I^- quenching of band 3-bound EMA was determined. As shown in Figure 4, it is found that the S-V plots become more linear as the temperature increases from 3 to 46 °C. Simulations based on eq 11 demonstrate that this is expected when K_d increases with increasing temperature. In the limit of no binding, the S-V plots revert to a linear form. Figure 4 also shows the best fits to the experimental data by eq 11. The values of the dissociation constant K_d and the apparent diffusion quenching constant K_q obtained from the fits are given in Table 1.

The increase in dissociation constant K_d with temperature indicates that binding of I^- to band 3 is an exothermic process. Increased temperature normally results in decreased stability of ligand−macromolecule complexes (Lakowicz, 1983). K_q also increases with temperature as expected for collisional quenching. We calculate the activation energy, E_a, for this process to be 3.6 kcal/mol, a value close to that for breaking hydrogen bonds (Fenichel & Horowitz, 1965). This might suggest that the diffusion pathway between the I^- binding site and EMA is aqueous in nature. However, the fluorescence lifetime of band 3-bound EMA is only about 10^{-9} s (Macara *et al.*, 1983). For quenching to occur, the I^- ion must reach the fluorophore within this time interval.

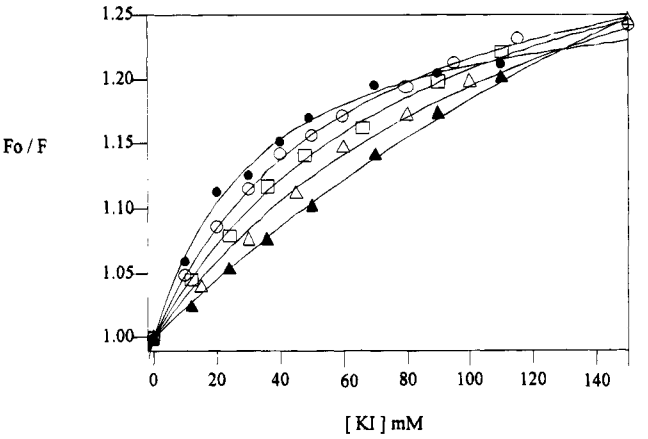

FIGURE 4: Temperature dependence of I^- quenching of band 3-bound EMA in ghosts: (●) 3 °C; (○) 12 °C; (□) 20 °C; (△) 30 °C; (▲) 46 °C. The lines were fitted to the data by eq 11 using a nonlinear least squares procedure. All measurements were in 5PB, and the ionic strength was maintained at 250 mM by addition of trisodium citrate. Samples were equilibrated at each temperature for 20 min prior to measurement.

Table 1: Temperature Dependence of Apparent Diffusion Quenching Constant K_q and Dissociation Constant K_d for I^- Binding to Band 3[a]

temp (°C)	K_q	K_d (mM)
3	0.28 (0.01)	23 (0.4)
12	0.35 (0.01)	45 (3)
20	0.39 (0.02)	63 (6)
30	0.44 (0.04)	89 (14)
46	0.78 (0.08)	181 (18)

[a] Parameters and SD (in parentheses) are obtained from fitting the data in Figure 3 by eq 11.

A mechanism whereby a bound I^- ion dissociates and diffuses to the probe would require a very high off-rate constant, in the order of 10^9 s^{-1}. An alternative mechanism is that bound I^- collides with the probe as a result of flexing motions of the protein. Such a mechanism has previously been postulated for fluorescence quenching of tryptophan in human serum albumin (Lehrer & Leavis, 1978). It should be noted that eq 11, which is used to analyze the present data, is not dependent on the details of the quenching mechanism within the pocket. The same equation will apply whenever the probability of quenching occurring is proportional to the concentration of bound quencher.

Figure 5 shows that change of the bulk solution viscosity by glycerol had no effect on the quenching reaction. If the fluorescence quenching reaction were a simple diffusion-controlled process, then the reaction rate would be expected to be inversely proportional to the viscosity. The absence of any viscosity dependence is consistent with the binding-diffusion model in which the collision step occurs within a pocket which is separate from the bulk phase and which does not experience the bulk phase viscosity. If the collision step involves flexing motions of the protein, then these must also be insensitive to the bulk aqueous phase viscosity.

Competition with DIDS and Other Anions. Quenching of band 3-bound EMA by I^- is inhibited by DIDS as shown in Figure 6. Fitting the S-V plots for different DIDS concentrations by eq 11 reveals that the apparent diffusion quenching constant K_q is insensitive to DIDS, but the dissociation constant K_d' increases linearly with DIDS concentration (insert in Figure 6). This is the expected result for competi-

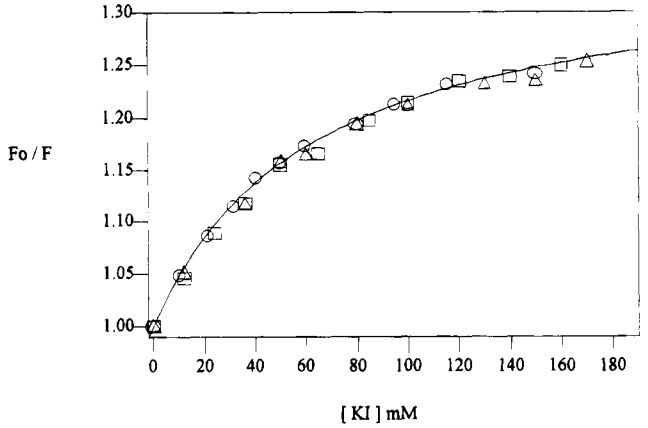

FIGURE 5: Effect of viscosity of the bulk solution on the quenching reaction between band 3-bound EMA and I^-: (○) 0% glycerol; (△) 35% glycerol; (□) 65% glycerol. The samples were in 5PB and the ionic strength was 250 mM. The temperature was 14 °C.

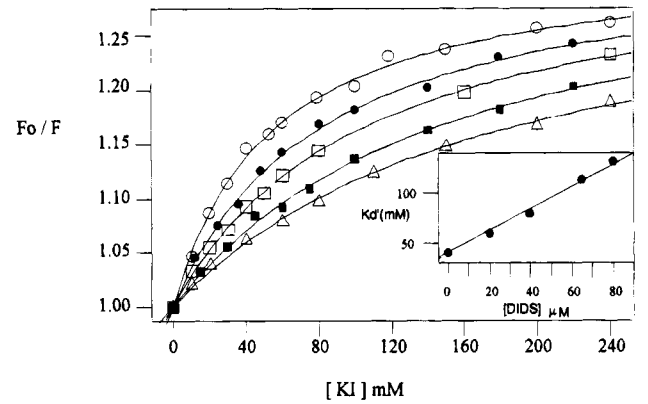

FIGURE 6: Effect of DIDS on I^- quenching of band 3-bound EMA. The lines were fitted to the data by eq 11 using a nonlinear least squares procedure. From top to bottom: [DIDS] = 0, 20, 40, 65, and 80 μM. The best-fit parameters were correspondingly $K_d' =$ 40, 60, 79, 114, and 132 mM and $K_q = 0.32$, 0.33, 0.33, 0.34, and 0.32. The inset shows a plot of K_d' against DIDS concentration. The line was fitted to the data by eq 17, yielding a value of K_d^A for DIDS binding to band 3 of 36 μM. All measurements were made at 14 °C in 5PB with an ionic strength of 250 mM.

tive binding of I^- and DIDS to the same site on band 3 (eq 17). From the slope of this plot, the dissociation constant for DIDS binding is determined to be 36 μM at 14 °C.

The above result may at first sight appear surprising since it is known that binding of stilbenedisufonate derivatives and EMA to band 3 are mutually exclusive. Covalent labeling of erythrocytes with DIDS protects band 3 from subsequent covalent labeling of EMA and *vice versa* (Nigg & Cherry, 1979; Macara *et al.*, 1983). In addition, strong interference between DIDS and EMA is observed under reversible binding conditions (0 °C; Knauf *et al.*, 1993). In the present experiments, however, we observed the effect of reversible binding of DIDS after EMA had been covalently bound to band 3. It has previously been shown that the covalently bound stilbenedisulfonate derivatives react with band 3 in two steps. Initial reversible binding is followed by covalent linkage to lysine on the 17 kDa fragment of band 3 (Bartel *et al.*, 1989a,b,; Salhany, 1990). A similar two-step reaction was also demonstrated for covalent binding of EMA to band 3 (Knauf *et al.*, 1993; Cobb & Beth, 1991). Thus the present results can be reasonably understood by supposing that covalently bound EMA does not prevent reversible binding of DIDS to band 3. The binding affinity for DIDS is, however, reduced as the K_d for DIDS in the absence of EMA is reported to be 31 nM (Janas et al., 1989).

Table 2: Apparent Dissociation Constants for Anion Binding to Band 3

anions	K_d for EMA-labeled band 3[a] (mM)	K_d for unlabeled band 3 (mM)
HCO_3^-	34 (3)	16,[b] 55 (4)[c]
I^-	41 (5)	10,[b] 34 (3)[c]
Br^-	67 (6)	32[b]
Cl^-	134 (11)	67,[b] 190[c]

[a] Values obtained at 14 °C from fluorescence quenching. [b] At 0 °C from Dalmark (1976). [c] From Falke *et al.* (1984) in the presence of 100 mM Cl^-.

We have also investigated the effects of the transportable anions Cl^-, Br^-, and HCO_3^- on I^- quenching of band 3-bound EMA fluorescence. None of these anions themselves exhibit any detectable quenching of EMA fluorescence (data not shown). Figure 7 shows the effect of Cl^-, HCO_3^-, and Br^- on the S-V plots for I^- quenching of band 3-bound EMA fluorescence. The ionic strength was held constant in these experiments by compensation with trisodium citrate which was previously used as a spectator anion in studies of the kinetics of band 3 mediated anion exchange (Milanick & Gunn, 1982; Gunn & Fröhlich, 1979; Knauf & Mann, 1986). As in the case of DIDS, analysis by eq 11 shows that the anions change K_d but not K_q. Plots of K_d' against anion concentration are linear (insets in Figure 7), indicative of competition for the I^- binding site. Values of the dissociation constants for the anions obtained from the slopes of these plots are given in Table 2.

It is worth noting that eq 11 can be rearranged to give

$$F/(F_0 - F) = (1 + 1/K_q)K_d'/[I^-] + 1/K_q \qquad (18)$$

where K_d' is given by eq 17 in the presence of a competing anion. Thus plots of $F/(F_0 - F)$ against $1/[I^-]$ are predicted to be linear with the intercept on the y axis of $1/K_q$. Figure 8 shows an example of such plots for competition by HCO_3^-. Similarly good agreement with eq 18 is obtained in the other competition experiments.

DISCUSSION

In the present paper, we show that the S-V plot for I^- quenching of band 3-bound EMA fluorescence exhibits downward curvature, a feature not observed when eosin is bound to other proteins. This result cannot be explained by direct quenching from the bulk aqueous phase but is consistent with a model in which the eosin probe is enclosed in a pocket within the protein. The concentration of quencher in the pocket is determined by specific binding to a site within the pocket.

It was previously found that I^- quenching of the triplet state of band 3-bound EMA gave rise to linear S-V plots (Wyatt & Cherry, 1992). Because of the long lifetime of the triplet state (~2 ms), triplet quenching experiments are performed at much lower I^- concentrations, typically 1−10 mM. Under these conditions, there is negligible equilibrium binding to the anion binding site, and hence the binding-diffusion model may not apply. The rate constant for triplet quenching is most likely determined by the probability of an I^- ion entering the pocket from the bulk phase during the lifetime of the eosin triplet state.

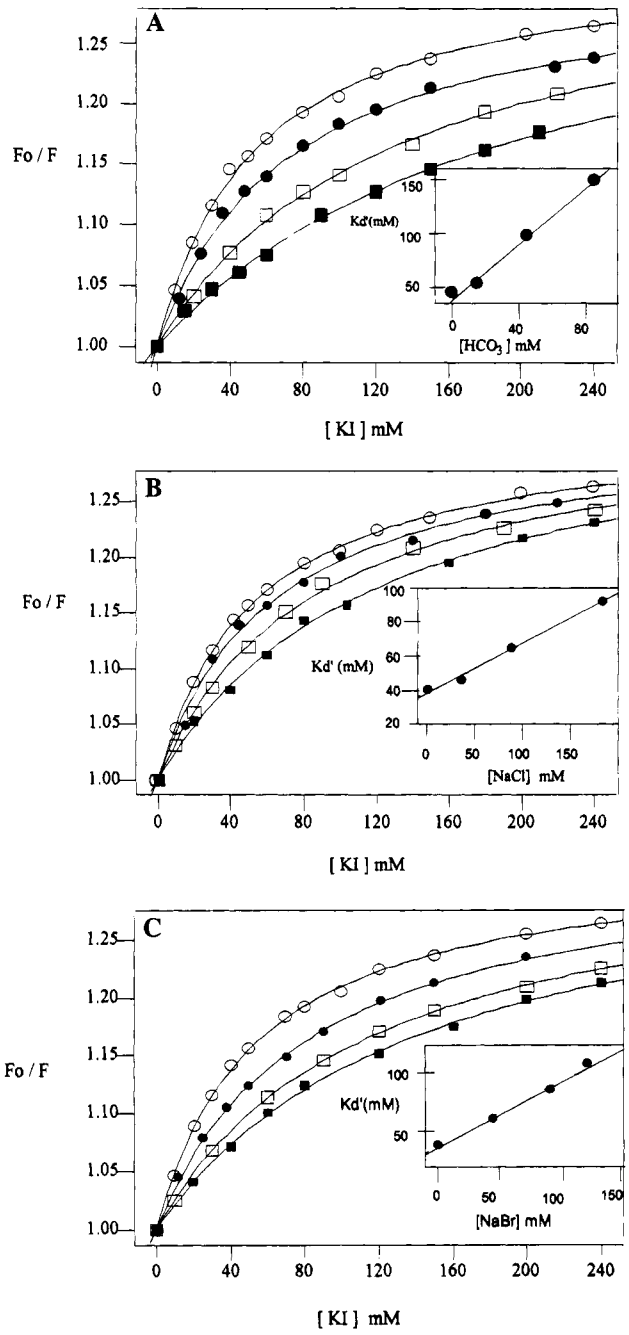

FIGURE 7: (A) Competitive inhibition of the quenching reaction between I^- and band 3-bound EMA by HCO_3^-. The lines were fitted to the data by eq 11 using a nonlinear least squares procedure. From top to bottom: $[HCO_3^-] = 0$, 15, 45, and 85 mM. The best-fit parameters were correspondingly $K_d' = 41$, 55, 98, and 149 mM and $K_q = 0.32$, 0.31, 0.33, and 0.34. The inset shows a plot of K_d' against $[HCO_3^-]$. The line was fitted to the data by eq 17, yielding $K_d^A = 34$ mM for HCO_3^-. (B) Competitive inhibition of the quenching reaction between I^- and band 3-bound EMA by Cl^-. The lines were fitted to the data by eq 11 using a nonlinear least squares procedure. From top to bottom: $[Cl^-] = 0$, 40, 90, and 180 mM. The best-fit parameters were correspondingly $K_d' = 41$, 47, 65, and 91 mM and $K_q = 0.33$, 0.32, 0.33, and 0.35. The inset shows a plot of K_d' against $[Cl^-]$. The line was fitted to the data by eq 17, yielding $K_d^A = 134$ mM for Cl^-. (C) Competitive inhibition of the quenching reaction between I^- and band 3-bound EMA by Br^-. The lines were fitted to the data by eq 11 using a nonlinear least squares procedure. From top to bottom: $[Br^-] = 0$, 45, 90, and 120 mM. The best-fit parameters were correspondingly $K_d' = 39$, 61, 86, and 108 mM and $K_q = 0.32$, 0.33, 0.33, and 0.34. The inset shows a linear plot of K_d' against $[Br^-]$. The line was fitted to the data by eq 17, yielding $K_d^A = 67$ mM for Br^-.

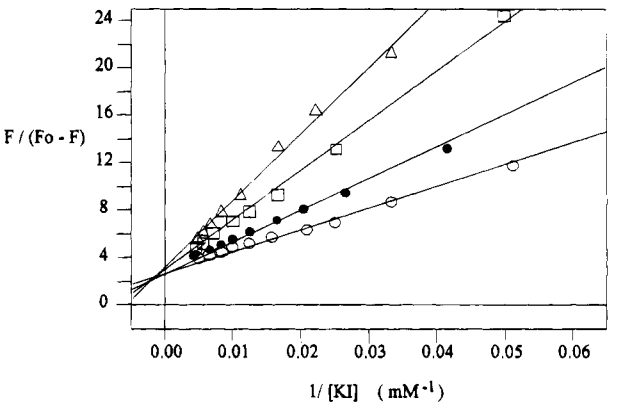

FIGURE 8: Data from Figure 7A replotted according to eq 18. From top to bottom: $[HCO_3^-] = 85$, 45, 15, and 0 mM.

The binding-diffusion model used to analyze the fluorescence quenching experiments requires no assumptions about the nature of the pocket in which the eosin probe is located. Because EMA is a potent inhibitor of anion transport, however, it has previously been argued that the probe is located in an access channel which forms part of the anion translocation pathway (Cobb & Beth, 1990; Nigg & Cherry, 1979; Macara *et al.*, 1983). Knauf *et al.* (1993), on the other hand, recently showed that eosin probes do not compete with anion binding to band 3 and hence proposed that EMA binds at a different site where it acts as a noncompetitive inhibitor of anion transport.

The present studies provide strong evidence that the pocket in which EMA is located and the anion access channel are one and the same entity. First, we show that DIDS, a competitive inhibitor of anion transport (Passow, 1986; Fröhlich & Gunn, 1987; Wojciki & Beth, 1993), competes at micromolar concentrations with the I^- binding site that controls fluorescence quenching of EMA. Second, we show that other transportable anions compete for the I^- site. Analysis of these competition experiments by the binding-diffusion model yields the dissociation constants given in Table 2. In Table 2 we also include K_d values obtained from anion-exchange kinetics (Dalmark, 1976) and from NMR experiments (Falke *et al.*, 1984). Comparison between these values is not entirely straightforward because the previous measurements are likely to include contributions from both inward and outward facing sites. Quenching of band 3-bound EMA fluorescence by I^-, however, probably only occurs from the side which is outward facing in intact cells (Wyatt & Cherry, 1992). It is nevertheless clear that there is reasonable agreement between our data and previous studies, both in the actual K_d values and in the order of binding strengths for the different anions. In addition, Knauf *et al.* (1992) reported an approximately 7-fold increase in K_d for I^- binding to the outward facing site between 0 and 38 °C. The K_d values in Table 1 show a very similar temperature dependence although the absolute values of K_d obtained by Knauf *et al.* are lower than those in Table 1. Overall, we are confident that the binding site which controls quenching of EMA fluorescence is the anion binding/transport site on band 3. We thus agree with recent studies (Knauf *et al.*, 1993; Liu *et al.*, 1994) which indicate that EMA does not itself compete for the anion binding site. It seems highly unlikely, however, that the compartment which EMA shares with the anion binding site on band 3 is any other than the anion access channel.

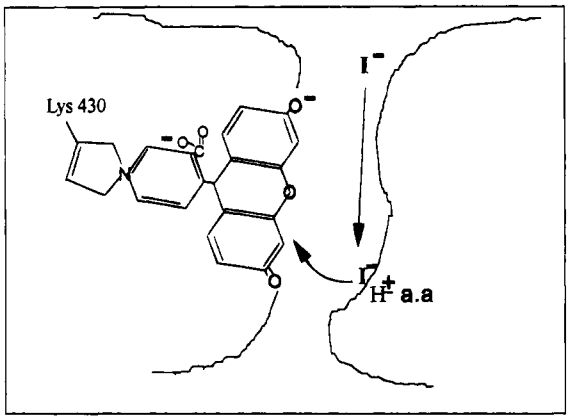

FIGURE 9: Schematic diagram of the anion access channel in band 3 showing the suggested location of EMA relative to the anion binding site (represented as a protonated amino acid residue).

The previous determinations of anion binding were performed with unmodified band 3 whereas the present studies require band 3 to be covalently modified with EMA. It is clear from Table 2 that labeling with EMA does not strongly perturb the anion binding site. It is possible, however, that EMA labeling does have some effect on the K_d values. This could occur either through an electrostatic effect arising from close proximity of eosin's negative charges or from an effect of eosin binding on band 3 conformation. There is evidence that there are some structural changes accompanying EMA binding to band 3 (Macara *et al.*, 1983; Batenjany *et al.*, 1993), although these would not necessarily affect the anion binding site.

Whereas previous studies find that I^- is the most tightly bound anion, the present experiments indicate that I^- binding is slightly weaker than bicarbonate. It may be that our determination of the K_d for I^-, which depends on analysis of absolute quenching, is less reliable than the determinations for the other anions which are obtained from competition experiments. It is also possible that the inhibitory effect of high anion concentration (Dalmark, 1976; Gunn & Fröhlich, 1979) affects our determination of the K_d for I^-. The dissociation constant for the inhibitory site for I^- (60 mM) is much lower than for the other anions (Dalmark, 1976).

EMA could inhibit anion exchange by blocking the access channel or by inhibiting the translocation step. Since the anion binding/transport site is generally believed to be at the base of the access channel, the lack of inhibition of anion binding by EMA suggests that the probe is most likely a translocation inhibitor. The shift in the absorbance maximum from 517 to 532 nm on binding to band 3 indicates that the probe is located in a mainly hydrophobic environment. We thus propose that EMA is buried in the wall of the access channel as shown schematically in Figure 9. In this location, it does not block the channel, but its outer electron shell is accessible to collisional quenchers in the access channel. In this model, insertion of the eosin ring system between amino acid residues in the wall of the channel allosterically inhibits the conformational change which occurs at the transport site during anion translocation.

In conclusion, the present study shows that fluorescence quenching experiments with EMA-labeled band 3 provide a simple method of studying the anion binding/transport site on band 3. In particular, they permit separation of anion binding and translocation. Although anion binding has previously been observed using ^{35}Cl NMR, this technique is not readily available to most workers. Fluorescence quenching experiments will enable anion binding to band 3 to be investigated under a variety of experimental conditions and, in particular, may help in the evaluation of the effects of mutagenesis on the anion transport function of band 3.

ACKNOWLEDGMENT

We are grateful to Dr. Paul O'Shea for generously making available the Ultrafit software and to I. E. G. Morrison for kindly providing EMA-labeled spectrin.

REFERENCES

Austin, R. H., Chan, S. S., & Jovin, T. M. (1979) *Proc. Natl. Acad. Sci. U.S.A. 76*, 5650−5654.
Bar-Noy, S., & Cabantchik, Z. I. (1990) *J. Membr. Biol. 115*, 217−228.
Bartel, D., Hans, H., & Passow, H. (1989a) *Biochim. Biophys. Acta 985*, 355−358.
Bartel, D., Lepke, S., Layh-Schmitt, G., & Passow, H. (1989b) *EMBO J. 8*, 3601−3609.
Batenjany, M. M., Mizukami, H., & Salhany, J. M. (1993) *Biochemistry 32*, 663−668.
Blatt, E., Chatelier, C., & Sawyer, W. H. (1986) *Biophys. J. 50*, 349−356.
Cabantchik, Z. I., BarNoy, S., Pollard, H. B., & Raviv, Y. (1992) *Prog. Cell Res. 2*, 51−58.
Casey, J. R., & Reithmeier, R. A. F. (1993) *Biochemistry 32*, 1172−1179.
Chalpin, D. B., & Kleinfeld, A. M. (1983) *Biochim. Biophys. Acta 731*, 465−474.
Cherry, R. J. (1978) *Methods Enzymol. 54*, 47−61.
Cherry, R. J. (1979) *Biochim. Biophys. Acta 559*, 289.
Cherry, R. J. (1992) in *Structural and Dynamic Properties of Lipids and Membranes* (Quinn, P. J., & Cherry, R. J., Eds.) pp 137−152, Portland Press, London.
Cobb, C. E., & Beth, A. H. (1990) *Biochemistry 29*, 8283−8290.
Dalmark, M. (1976) *J. Gen. Physiol. 67*, 223−234.
Dalmark, M., & Wieth, J. O. (1972) *J. Physiol. (London) 224*, 583−610.
Dix, J. A., Verkman, A. S., & Solomon, A. K. (1986) *J. Membr. Biol. 89*, 211−223.
Eftink, M. R. (1991) in *Topics in Fluorescence Spectroscopy* (Lakowicz, J. R., Ed.) Vol. 2, pp 53−126, Plenum, New York.
Eftink, M. R., & Hagaman, K. A. (1987) *Biophys. Chem. 26*, 277−282.
Eidelman, O., Yanai, P., Lang, H. C., Lang, H. G., Greger, R., & Catbanchick, Z. I. (1991) *Am. J. Physiol. 260*, C1094−C1103.
Falke, J. J., Pace, R. J., & Chan, S. I. (1984) *J. Biol. Chem. 259*, 6472−6480.
Fenichel, R., & Horowitz, S. B. (1965) *Ann. N.Y. Acad. Sci. 125*, 290−297.
Fröhlich, O. (1992) *J. Membr. Biol. 65*, 111−123.
Fröhlich, O., & Gunn, R. B. (1987) *Am. J. Physiol. 252*, C153−C162.
Garcia, A., & Lodish, H. (1989) *J. Biol. Chem. 264*, 19607−19613.
Gunn, R. B., & Fröhlich, O. (1979) *J. Gen. Physiol. 74*, 351−374.
Hamasaki, N., Izuhara, K., & Okubo, K. (1989) in *Anion Transport Protein of the Red Blood Cell Membrane* (Hamasaki, M., & Jennings, M. L., Eds.) p 47, Elsevier, Amsterdam.
Janas, T., Bjerrum, P. J., Brahm, J., & Wieth, J. O. (1980) *Am. J. Physiol.* 257, C601−C606.
Jennings, M. L. (1984) *J. Membr. Biol. 80*, 105−117.
Jennings, M. L. (1985) *Annu. Rev. Physiol. 47*, 519−533.
Jennings, M. L. (1989) in *Anion Transport Protein of the Red Blood Cell Membrane* (Hamasaki, M., & Jennings, M. L., Eds.) pp 59−72, Elsevier, Amsterdam.
Jennings, M. L., & Passow, H. (1979) *Biochim. Biophys. Acta 554*, 498−519.
Jennings, M. L., & Anderson, R. M. (1987) *J. Biol. Chem. 262*, 1691−1697.

Jennings, M. L., Adams-Lacky, M., & Denny, G. H. (1984) *J. Biol. Chem. 259*, 4652−4660.
Julien, T., & Zaki, L. (1988) *J. Membr. Biol. 102*, 217−224.
Kaplan, J. H., Scorah, K., Fasold, H., Pring, M., & Passow, H. (1976) *FEBS Lett. 62*, 182−185.
Knauf, P. A. (1979) *Curr. Top. Membr. Transp. 12*, 249−363.
Knauf, P. A., & Mann, N. (1986) *Am. J. Physiol. 251*, C1−C9.
Knauf, P. A., Restrepo, D., Liu, S. J., Raha, N. M., Spinelli, L. J., Law, Y. J., Cronise, B., Snyder, R. B., & Romanov, L. (1992) *Prog. Cell Res. 2*, 35−44.
Knauf, P. A., Strong, N. M., Penikas, J., Wheeler, R. B., Jr., & Liu, S. J. (1993) *Am. J. Physiol. 164*, C1144−C1154.
Kopito, R. R., & Lodish, H. F. (1985) *Nature (London) 316*, 234−238.
Lakowicz, J. R. (1983) in *Principles of Fluorescence Spectroscopy*, p 265, Plenum, New York.
Lehrer, S. S. (1971) *Biochemistry 10*, 3254−3263.
Lehrer, S. S., & Leavis, P. C. (1978) *Methods Enzymol. 49*, 222−236.
Liu, S. J., & Knauf, P. A. (1993) *Am. J. Physiol. 264*, C1155−C1164.
Liu, D., Kennedy, S., & Knauf, P. A. (1994) *Biophys. J. 66*, A337.
Low, P. S. (1986) *Biochim. Biophys. Acta 864*, 145−167.
Lowry, O. H., Rosebrough, N. J., Farr, A. L., & Randall, R. J. (1951) *J. Biol. Chem. 193*, 265−275.
Macara, I. G., & Cantley, L. C. (1981) *Biochemistry 20*, 5095−5105.
Macara, I. G., Kuo, S., & Cantley, L. C. (1983) *J. Biol. Chem. 258*, 1785−1792.
Milanick, M. A., & Gunn, R. B. (1982) *J. Gen. Physiol. 79*, 87−113.
Nigg, E. A., & Cherry, R. J. (1979) *Biochemistry 18*, 3457−3465.
Nigg, E., Kessler, M., & Cherry, R. J. (1979) *Biochim. Biophys. Acta 50*, 328−340.
Okubo, K., Kang, D., Hamasaki, N., & Jennings, M. L. (1994) *J. Biol. Chem. 269*, 1918−1926.
Passow, H. (1986) *Rev. Physiol. Biochem. Pharmacol. 103*, 61−203.
Passow, H., Lepke, S., & Wood, P. G. (1992) Prog. Cell Res. *2*, 85−98.
Rao, A., Martin, P., Reithmeier, R. A. F., & Cantley, L. L. C. (1979) *Biochemistry 18*, 4505−4516.
Reithmeier, R. A. F. (1993) *Curr. Opin. Struct. Biol. 3*, 515−523.
Salhany, J. M. (1990) in *Erythrocyte Band 3 Protein*, CRC Press, Boca Raton, FL.
Salhany, J. M., Rauenbuehler, P. B., & Sloan, R. L. (1987) *J. Biol. Chem. 262*, 15965−15973.
Salhaney, J. M., Sloan, R. L., Cordes, K. A., & Schopfer, L. M. (1994) *Biochemistry 33*, 11909−11916.
Shami, Y., Rothstein, A., & Knauf, P. A. (1978) *Biochim. Biophys. Acta 508*, 357−363.
Tanner, M. J. A., Martin, P. G., & High, S. (1988) *Biochem. J. 256*, 703−712.
Thulborn, K. R., & Sawyer, W. (1978) *Biochim. Biophys. Acta 511*, 125−140.
Tilley, L., & Sawyer, W. H. (1992) *Comments Mol. Cell. Biophys. 7*, 333−352.
Van Veen, M., & Cherry, R. J. (1992) *FEMS Microbiol. Immunol. 105*, 147−150.
Wasylewski, Z., Koloczek, H., & Wasniowska, A. (1988) *Eur. J. Biochem. 172*, 719−724.
Wojciki, W. E., & Beth, A. H. (1993) *Biochemistry 32*, 9454−9464.
Wood, P. G. (1992) *Prog. Cell Res. 2*, 325−338.
Wood, P. G., Müller, H., Sovaka, M., & Passow, H. (1992) *J. Membr. Biol. 127*, 139−148.
Wyatt, K., & Cherry, R. J. (1992) *Biochemistry 31*, 4650−4656.

BI9418380